

SUPPLEMENTARY MATERIAL

Phase behavior of palmitoyl and egg sphingomyelin

Zoran Arsov*¹, Emilio J. González-Ramírez*², Felix M. Goñi²,
Stephanie Tristram-Nagle³ and John F. Nagle^{3,+}

¹*Department of Condensed Matter Physics, Laboratory of Biophysics, Jozef Stefan Institute,
1000 Ljubljana, Slovenia*

²*Instituto Biofísica (CSIC, UPV/EHU) and Departamento de Bioquímica, Universidad del País
Vasco, 48080 Bilbao, Spain*

³*Biological Physics Group, Physics Department, Carnegie Mellon University, 5000 Forbes
Avenue, Pittsburgh, Pennsylvania 15213*

**Contributed equally as first co-authors*

+Corresponding author

The figures on pages S2-6 are 2D CCD images of hydrated, oriented egg sphingomyelin (ESM) collected as a function of temperature using the Rigaku RUH3R with Xenocs focusing collimator as described in the Materials and Methods in the main paper. These data are the evidence that ESM remains in the ripple phase at all temperatures between 3 and 35 °C, since all of the images contain off-specular reflections characteristic of the ripple phase as shown in Fig. 1 in the main paper. While Fig. S1 is a summary figure of all of the ESM data images, Figs. S2-8 are individual 2D CCD images at each temperature for viewing at higher resolution. Units on images are detector pixels, Δq of $1.0 \text{ \AA}^{-1} \approx 650$ pixels.

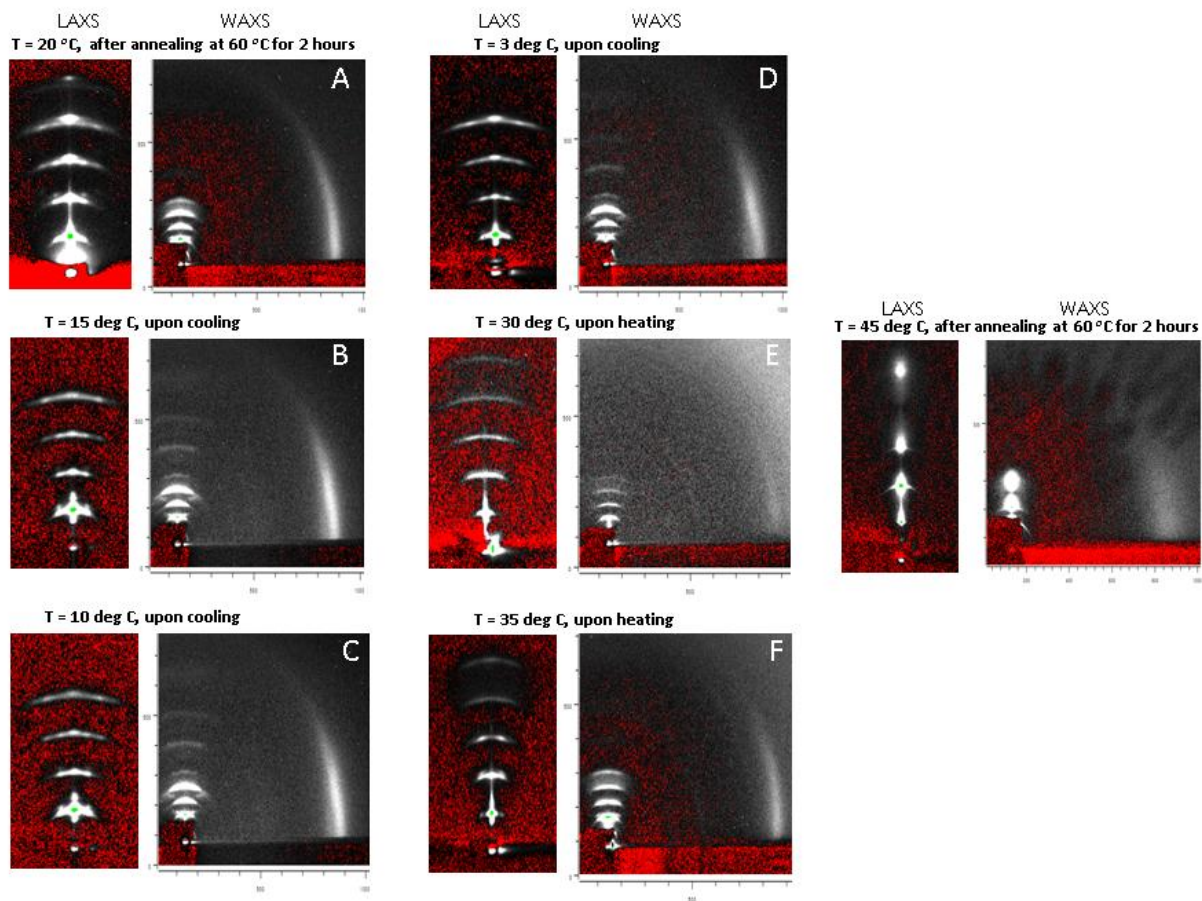
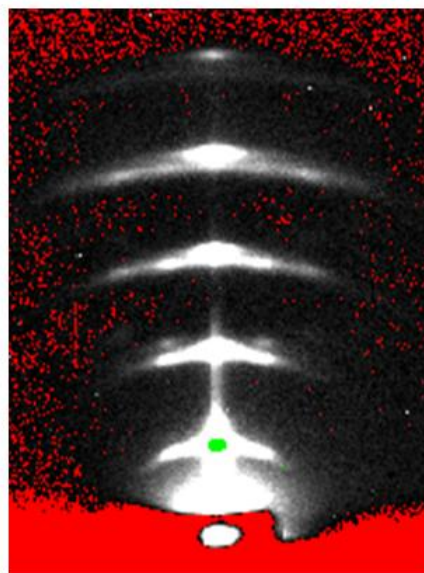


Figure S1. 2D CCD X-ray scattering data from oriented, hydrated ESM collected at the following temperatures: Ripple phase A. 20 °C, after annealing at 60 °C for 2 hours, B. 15 °C, upon cooling from 20 °C, C. 10 °C, upon cooling from 15 °C, D. 3 °C, upon cooling from 10 °C, E. 30 °C, upon heating from 3 °C, F. 35 °C, upon heating from 30 °C, Fluid phase G. 45 °C, after annealing at 60 °C for 2 hours. Red pixels indicate negative intensity after background subtraction.

LAXS



WAXS

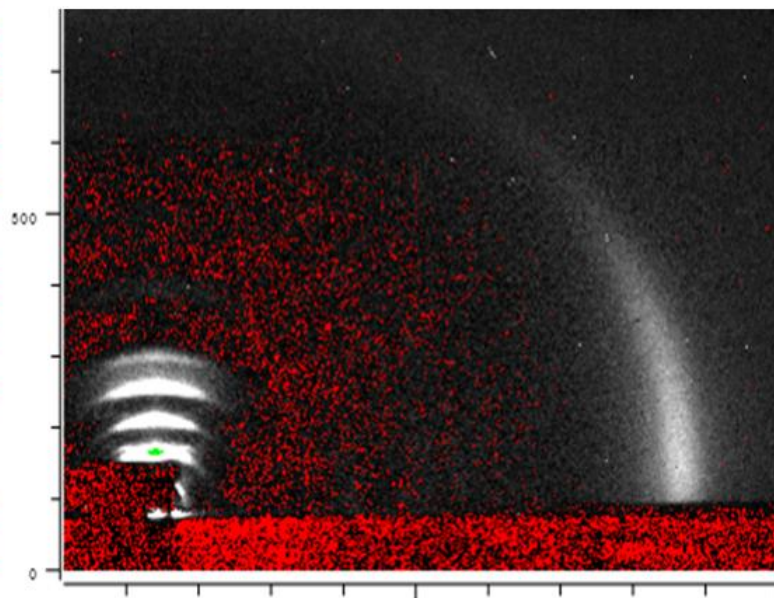
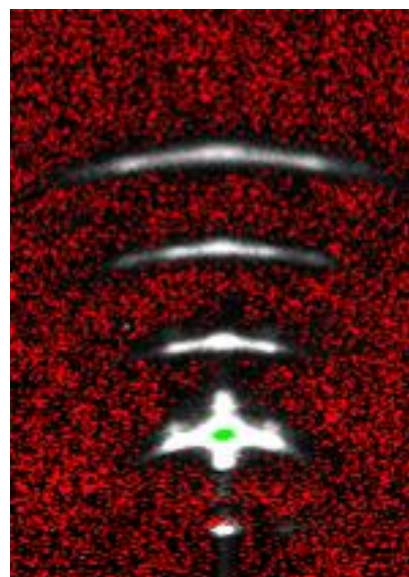


Figure S2. Oriented ESM at 20 °C in the ripple phase, collected after annealing at 60 °C for 2 hours. D-spacing is $64.9 \pm 0.9 \text{ \AA}$.

LAXS



WAXS

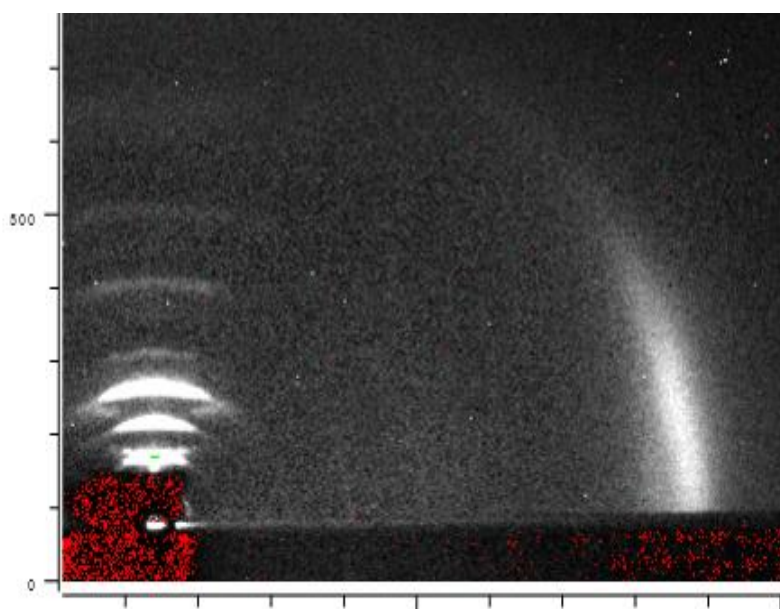
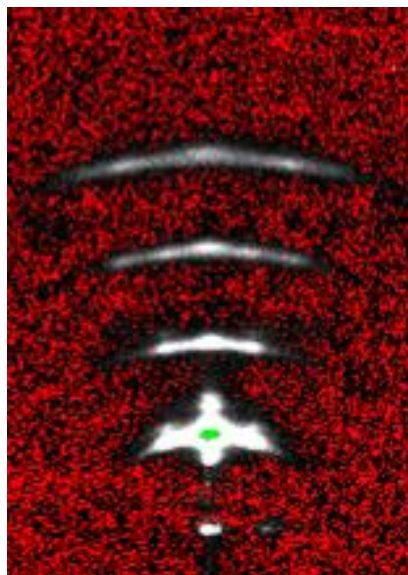


Figure S3. Oriented ESM at 15 °C in the ripple phase, collected after cooling from 20 °C. D-spacing is $60.8 \pm 0.8 \text{ \AA}$.

LAXS



WAXS

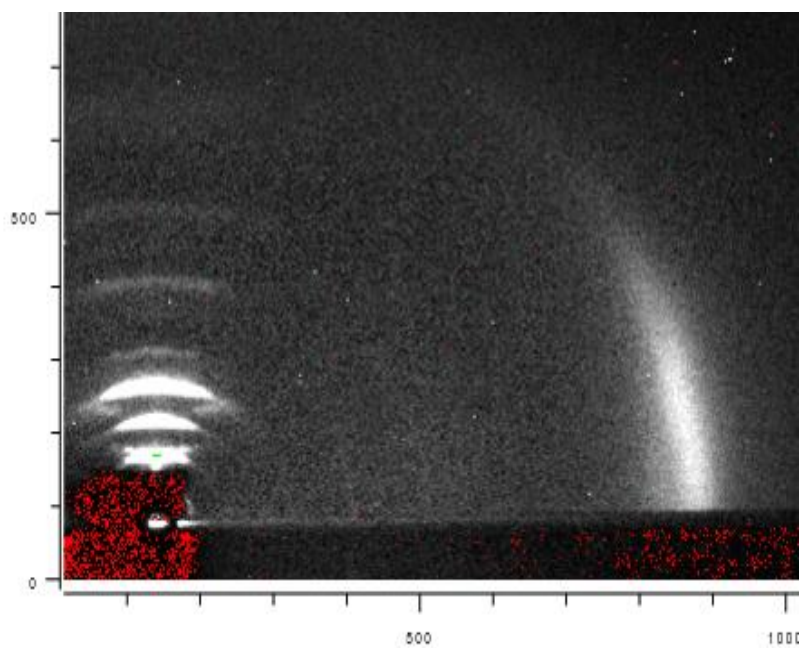
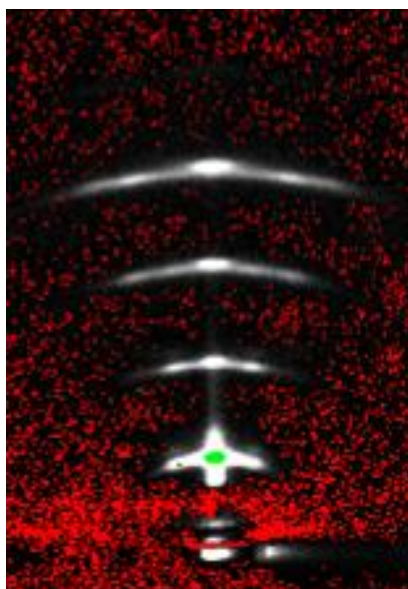


Figure S4. Oriented ESM at 10 °C in the ripple phase, collected after cooling from 15 °C. D-spacing is 60.8 ± 0.8 Å.

LAXS



WAXS

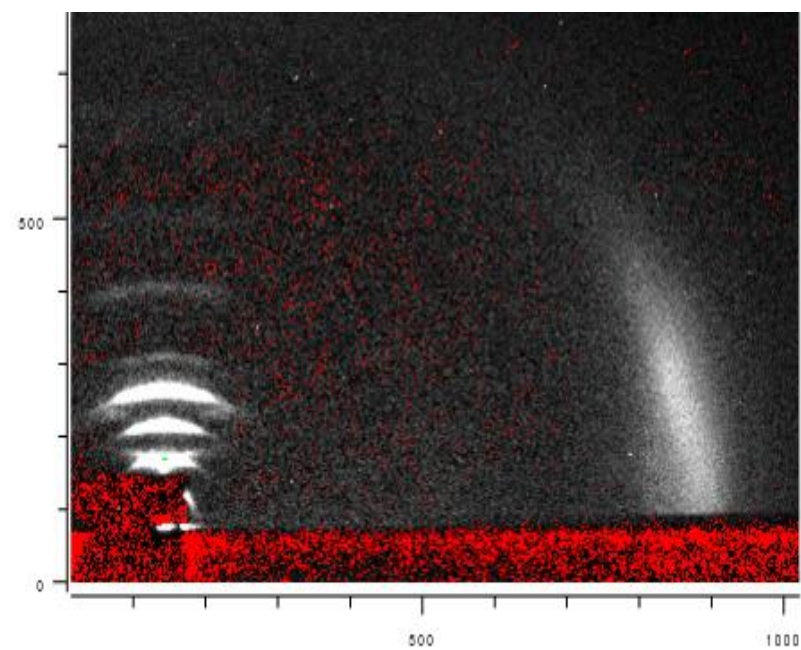
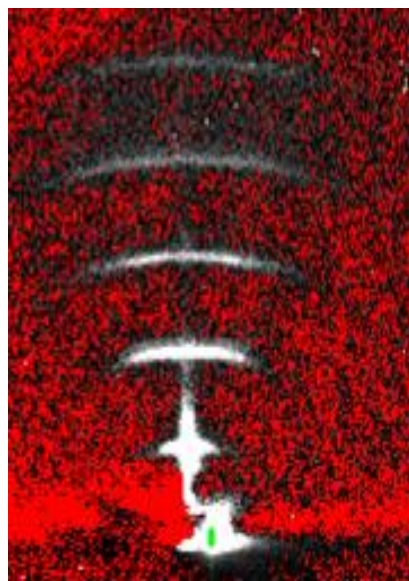


Figure S5. Oriented ESM at 3 °C in the ripple phase, collected after cooling from 10 °C. D-spacing is 60 ± 0.2 Å.

LAXS



WAXS

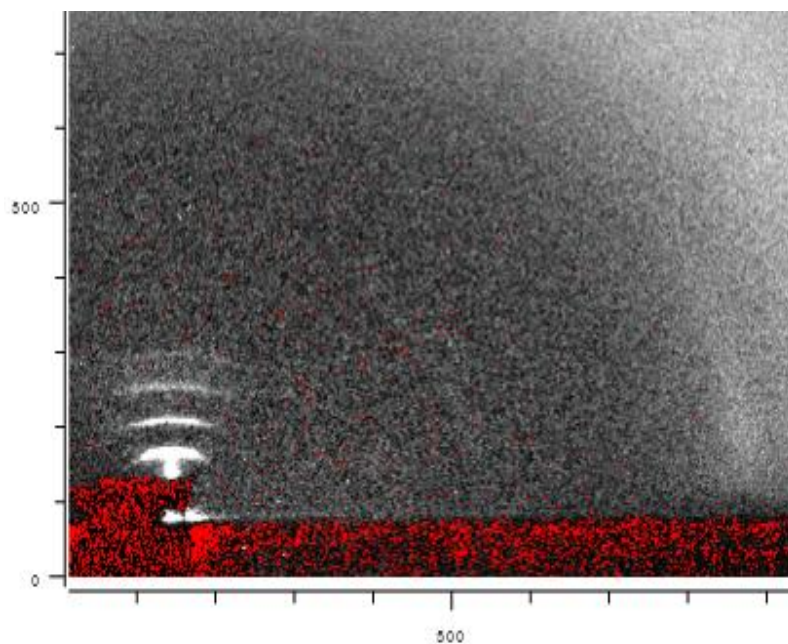
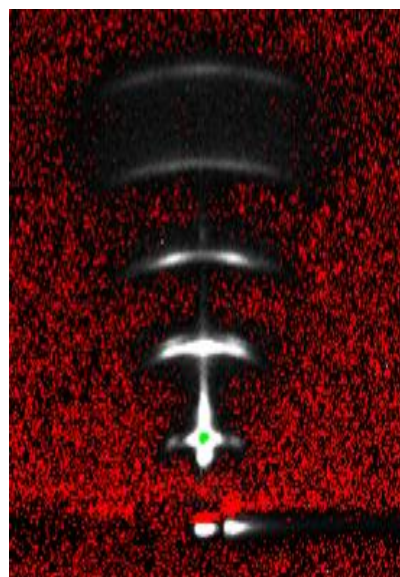


Figure S6. Oriented ESM at 30 °C in the ripple phase, collected after heating from 3 °C. D-spacing is 65 Å. The light, diffuse scattering in the upper right hand corner of the WAXS image is due to excess water on the sample.

LAXS



WAXS

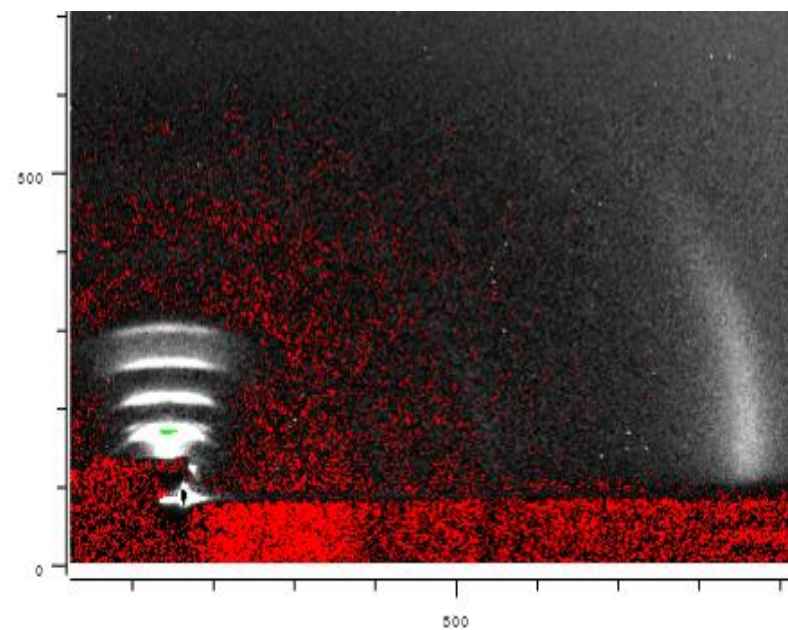
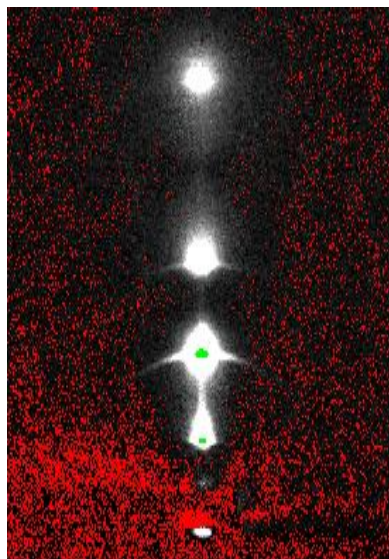


Figure S7. Oriented ESM at 35 °C in the ripple phase, collected after heating from 30 °C. D-spacing is 65.8 ± 1.2 Å.

LAXS



WAXS

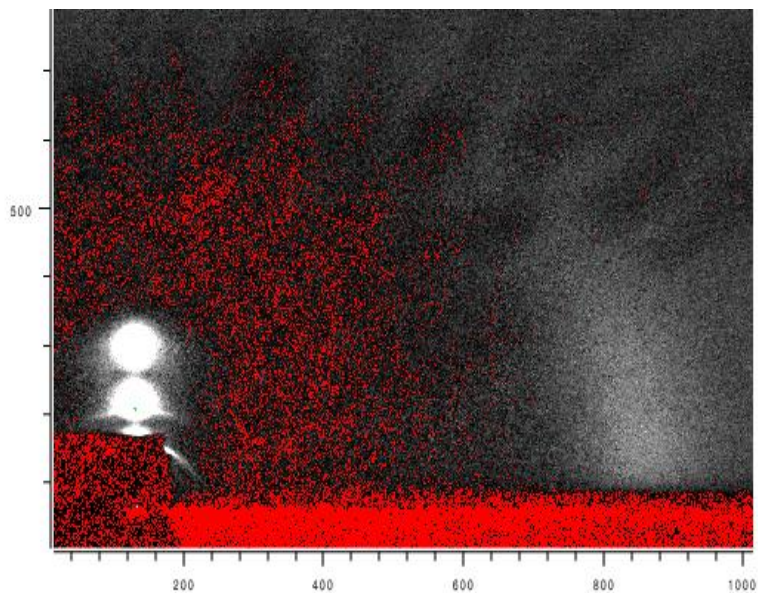


Figure S8. Oriented ESM at 45 °C in the fluid phase, collected after annealing at 60 °C for 2 hours. At 45 °C, SPM is in the fluid phase, as evidenced by the absence of ripple reflections in LAXS and broad, diffuse scattering in WAXS. D-spacing is $62.7 \pm 1.1 \text{ \AA}$.

The figures on pages S7-10 are 2D CCD images of hydrated, oriented palmitoyl sphingomyelin (PSM) collected as a function of temperature using the Rigaku RUH3R with Xenocs focusing collimator as described in the Materials and Methods in the main paper. These data are the evidence that PSM undergoes a phase transition from the gel phase to the ripple phase between 24 and 30 °C and then melts into the fluid phase between 37 and 45 °C as evidenced by reflections characteristic of these three phases. While Fig. S9 is a summary figure of all of the PSM data images, Figs. S10-15 are individual 2D CCD images at each temperature for viewing at higher resolution.

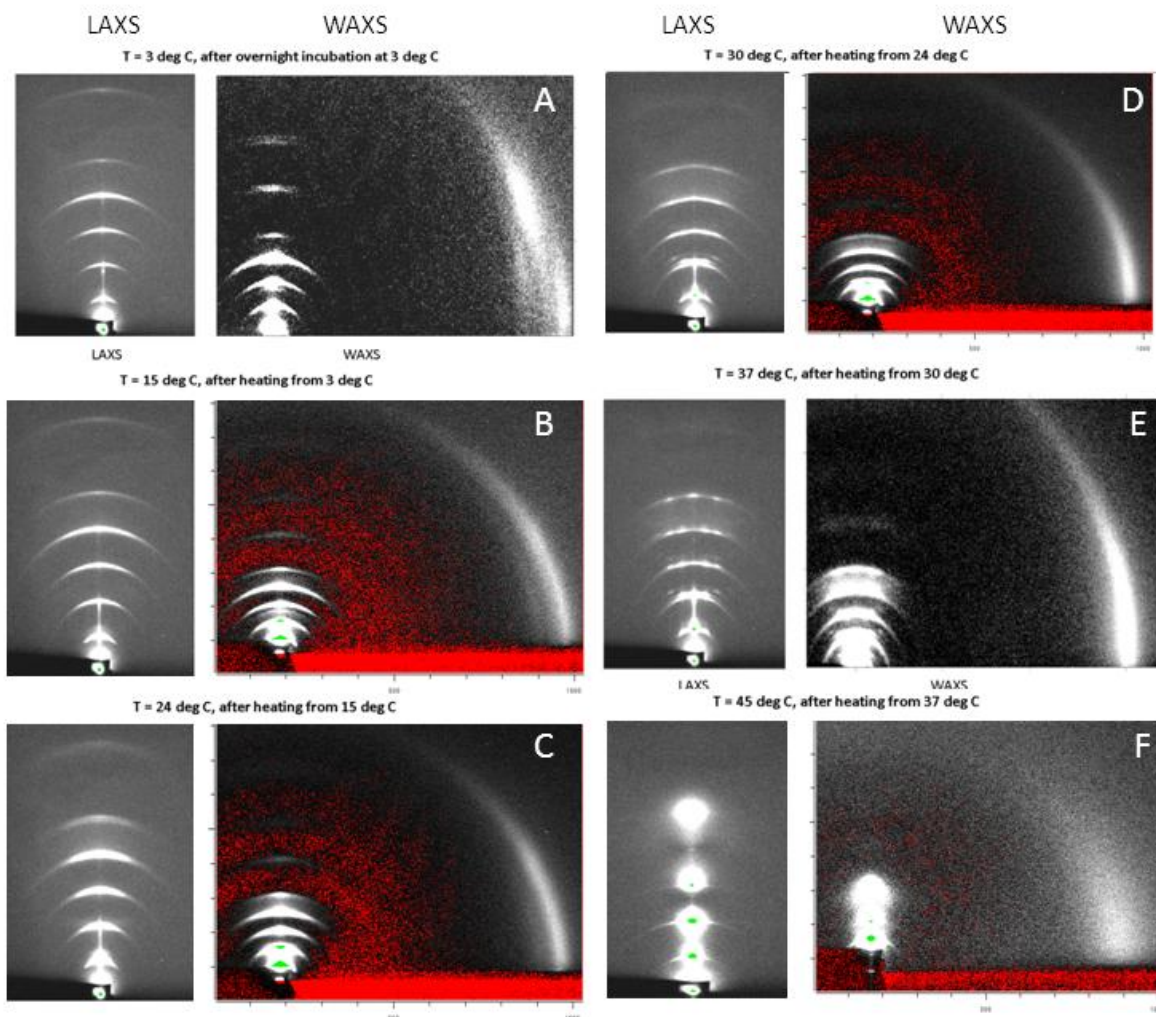


Figure S9. 2D CCD X-ray scattering data from oriented, hydrated PSM collected at the following temperatures: Gel phase: A. 3 °C, upon cooling from 37 °C and equilibrating overnight at 3 °C, B. 15 °C, upon heating from 3 °C, C. 24 °C, upon heating from 15 °C, Ripple phase: D. 30 °C, upon heating from 24 °C, E. 37 °C, upon heating from 24 °C, Fluid phase: F. 45 °C, upon heating from 37 °C.

T = 3 deg C, after overnight incubation at 3 deg C

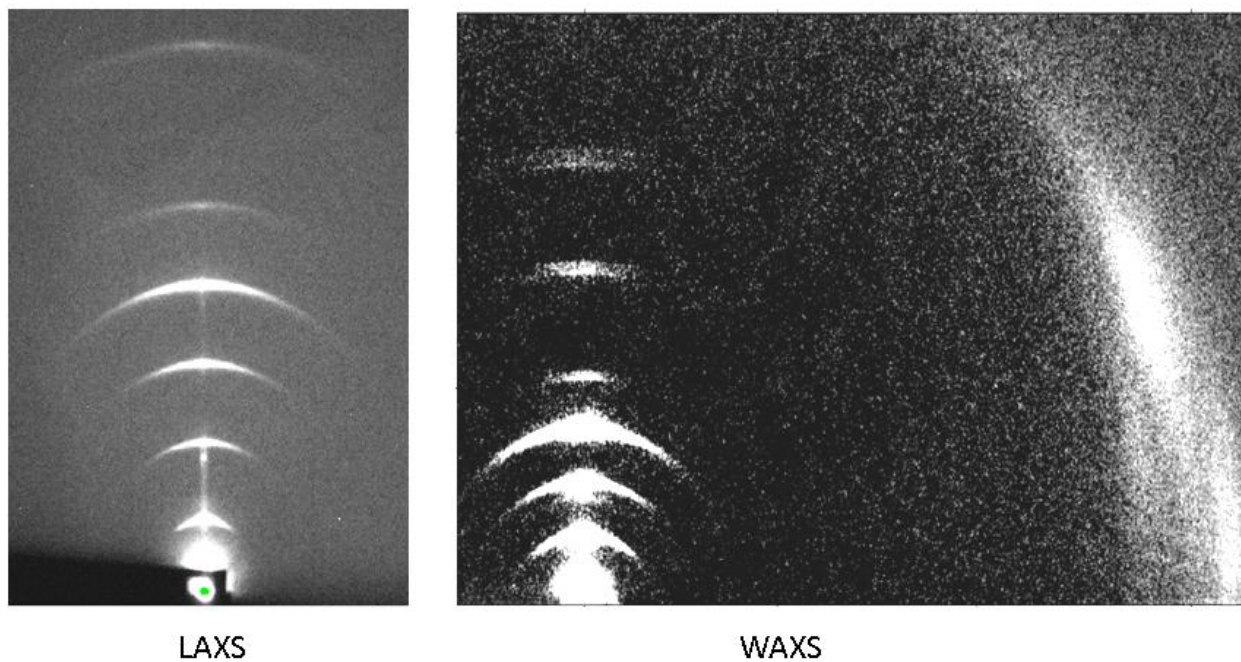


Figure S10. Oriented PSM at 3 °C in the gel phase, collected after cooling from 37 °C and equilibrating overnight at 3 °C. D-spacing is 60 ± 0.2 Å.

T = 15 deg C, after heating from 3 deg C

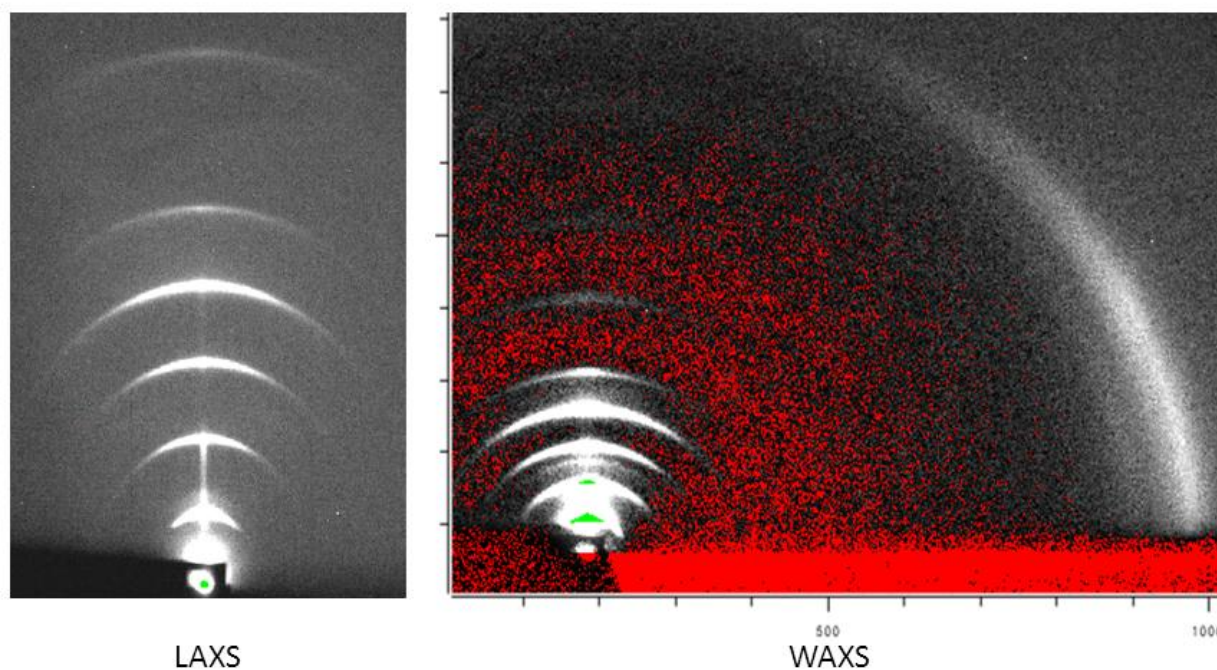


Figure S11. Oriented PSM at 15 °C in the gel phase, collected after heating from 3 °C. D-spacing is 60.6 ± 0.3 Å.

T = 24 deg C, after heating from 15 deg C

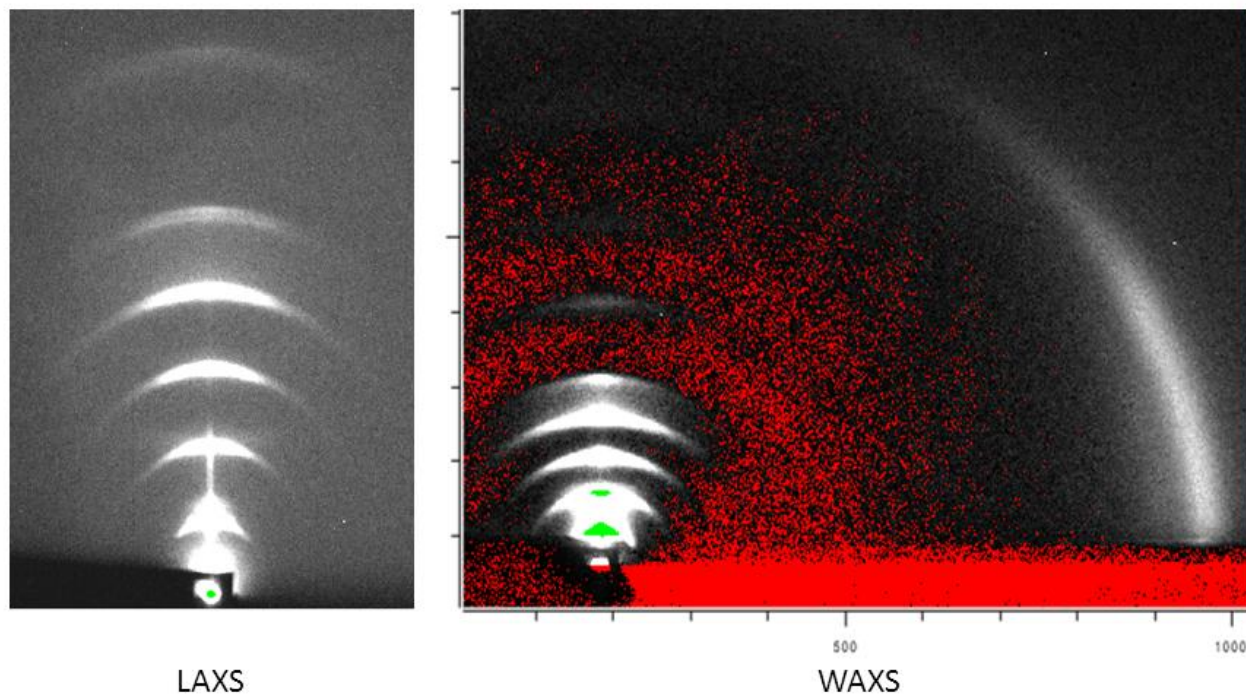


Figure S12. Oriented PSM at 24 °C gel phase with incipient ripple phase, collected after heating from 15 °C. D-spacing is $61 \pm 0.3 \text{ \AA}$.

T = 30 deg C, after heating from 24 deg C

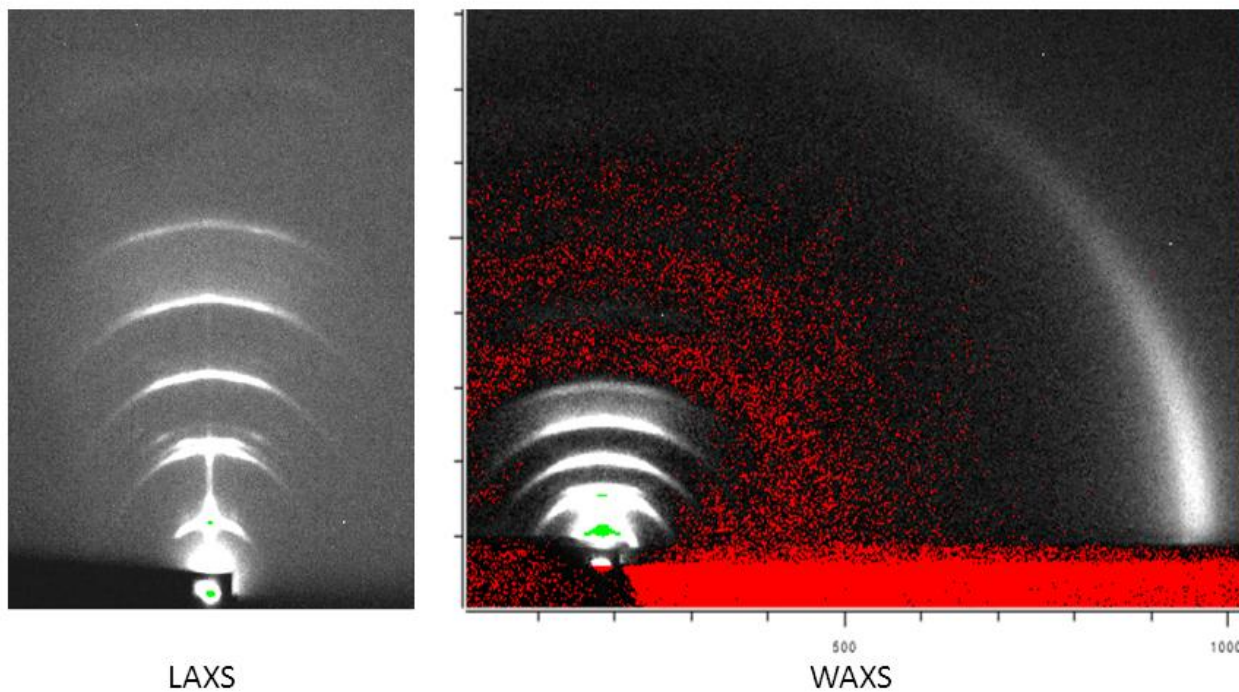


Figure S13. Oriented PSM at 30 °C in the ripple phase, collected after heating from 24 °C. D-spacing is $63.2 \pm 0.2 \text{ \AA}$.

T = 37 deg C, after heating from 30 deg C

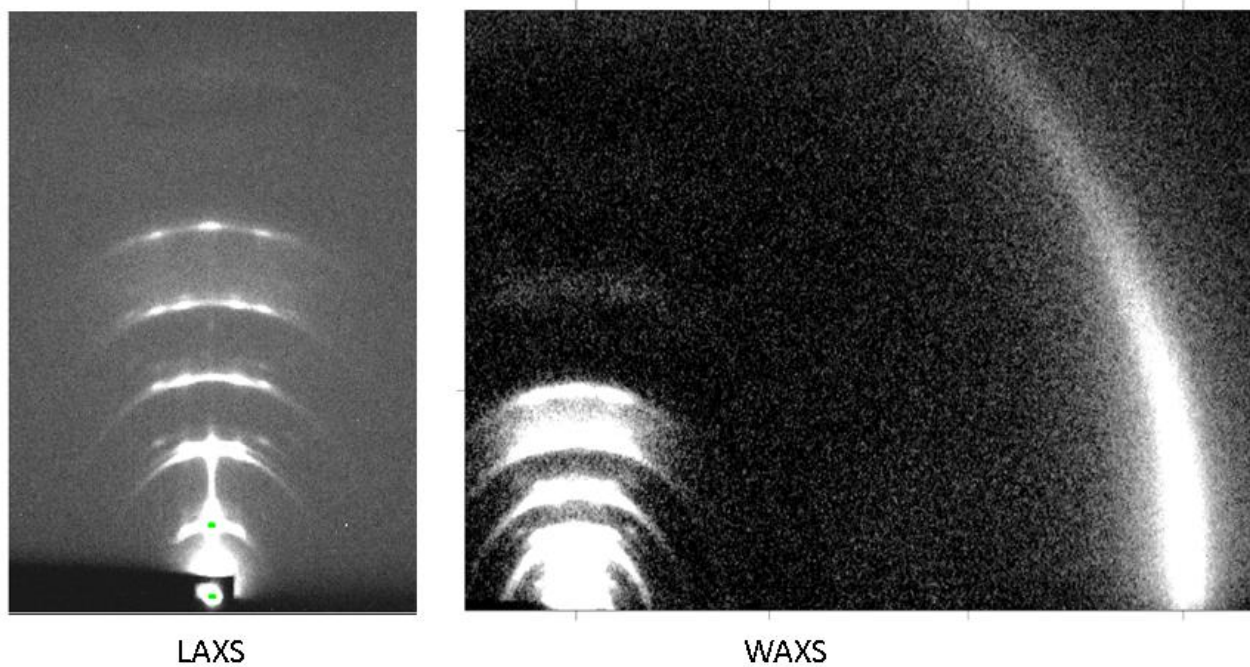


Figure S14. Oriented PSM at 37 °C in the ripple phase, collected after heating from 30 °C. D-spacing is $63.6 \pm 0.8 \text{ \AA}$.

T = 45 deg C, after heating from 37 deg C

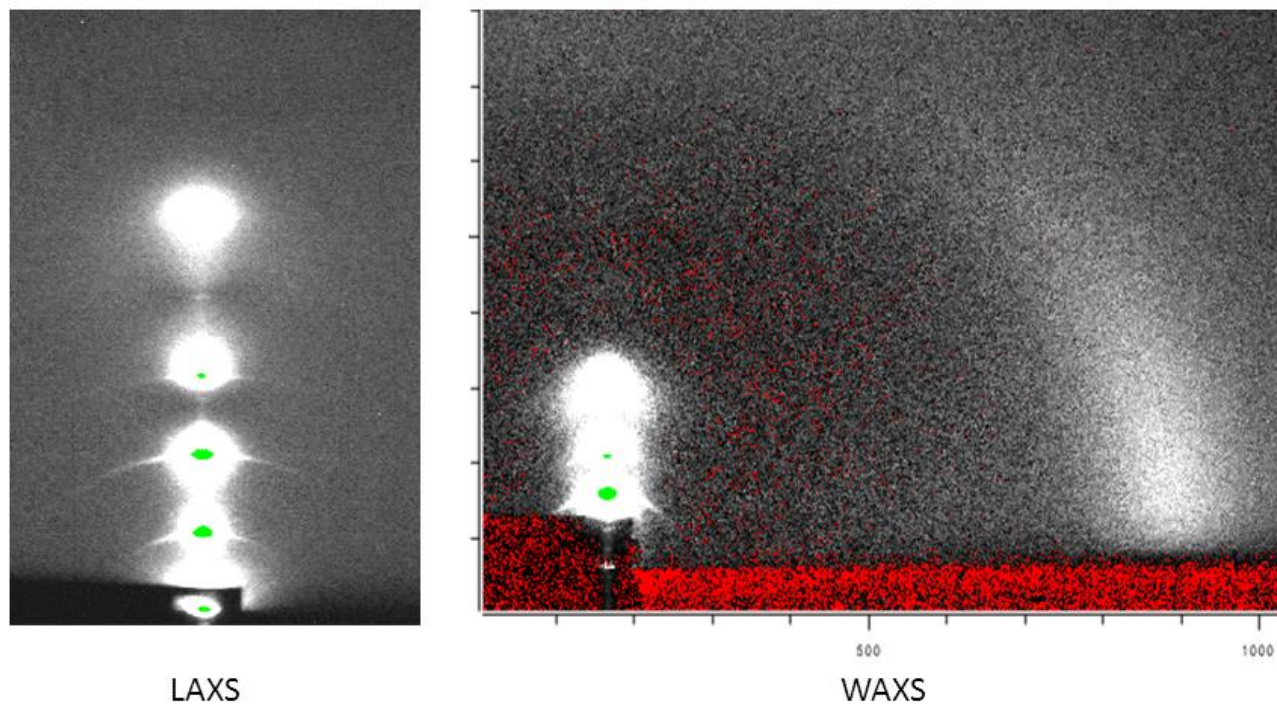


Figure S15. Oriented PSM at 45 °C in the fluid phase, collected after heating from 37 °C. D-spacing is $61.9 \pm 0.2 \text{ \AA}$.

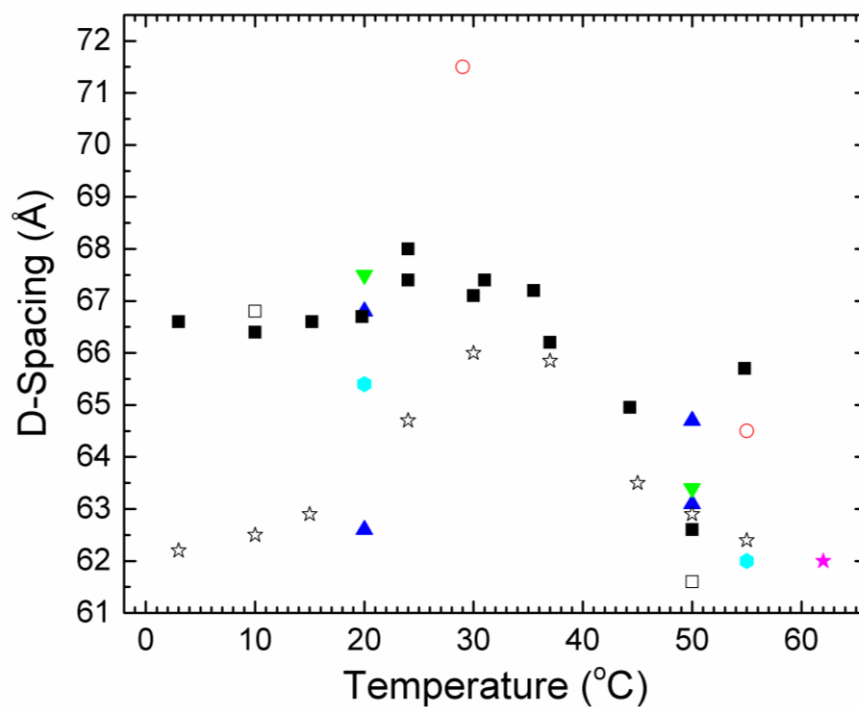


Figure S16. Capillary D-spacings from literature: **PSM**, open black squares (Calhoun and Shipley, 1979a), open red circles (Maulik and Shipley, 1996), open black stars (ThisWork, 2018); **ESM**, solid green inverted triangles (Chachaty et al., 2005), solid blue triangles (Quinn and Wolf, 2009), solid cyan hexagons (Chemin et al., 2008), solid magenta star (Shaw et al., 2012), solid black squares (ThisWork, 2018) .

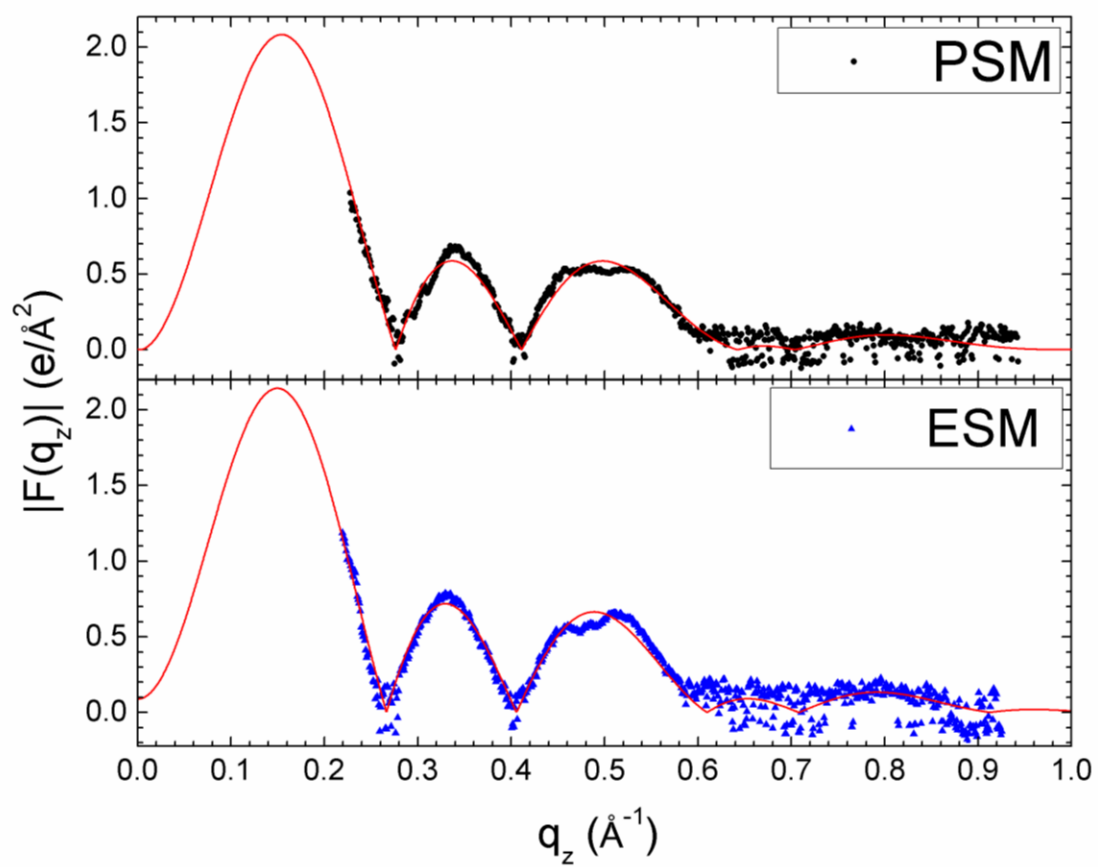


Figure S17. Form factor data obtained from x-ray diffuse scattering used to obtain the EDPs shown in Fig. 11 in the main paper.

Table S1. Literature phase transition DSC results

PSM				Heating rate	
Reference	Pretransition	T_P (°C)	T_M (°C)	(°C/h)	Material
(Barenholz and Shinitzky, 1976)	Probably	25	41.3	15	[†]
(Barenholz et al., 1976)	Yes	25	41.3	3-50	[†]
(Calhoun and Shipley, 1979a)	Yes (small)	31	40.5	300	D,L*
(Ahmad et al., 1985)	No	---	41.5	150/300	[†]
(Sripada et al., 1987)	No	---	41.0	300	D,L*
(Maulik and Shipley, 1996)	No	---	41.0	300	D,L*
(Bar et al., 1997)	Yes (small)	29.6	41.1	20	Lipitek
(Ramstedt and Slotte, 1999)	Yes (small)	28.9	41.1	18	D-erythro
(Ramstedt and Slotte, 1999)	No	---	39.9	18	Racemic, D,L*
(Chemin et al., 2008)	No	---	45	120	D-erythro
(Kodama et al., 2012)	Yes (small)	27.5	40.4	45	D-erythro
(Jimenez-Rojo et al., 2014)	Yes	30.9	41.7	45	Avanti
(Nyholm et al., 2003)	Yes	27.4	40.9	30	D-erythro
(Estep et al., 1979)	No	---	41	15	[†]
ESM					
(Calhoun and Shipley, 1979a)	No	---		300	Avanti
(Ahmad et al., 1985)	No	---	39-40	150/300	Sigma
(Mckeone et al., 1986)	No	---	37.7	30	Avanti
(Chien et al., 1991)	No	---	37.5	300	Avanti
(Mannock et al., 2003)	No	---	39.1	10	Avanti
(Filippov et al., 2006)	No	---	38.8	20	Avanti
(Chemin et al., 2008)	No	---	39.3	30	Avanti
(Jimenez-Rojo et al., 2014)	Yes?	---	38.1	45	Avanti
(Garcia-Arribas et al., 2016)	No	---	36	45	Avanti

[†]Possible stereospecificity is lacking

*D,L = D-erythro, L-threo SM

Table S2. Summary of structural parameters from PSM experiments

	T (°C)	D _{PP} (Å)	A _L (Å ²)	Volume (Å ³)	D _B (Å)	D _C (Å)	Tilt (°)	d-space (Å)	<S _{CD} >
(Calhoun and Shipley, 1979b)	10		54.8*		38.4*		47*	4.14	
	50		59.4*		35.4*			4.6	
(Maulik et al., 1986)	50	36.5	64.3*	1173*					
(Maulik and Shipley, 1996)	29	48	41*	1103*	54*			4.2	
	55	42	46*	1181*	51*			4.6	
(Li et al., 2000) (monolayer)	10		46.3						
(Mehnert et al., 2006)	< 30						0		
	48								0.258
	48								0.214 (DPPC)
	3 (DPPC)	---	47.0 (DPPC)	1128 (DPPC)	48 (DPPC)	---	34 (DPPC)	4.27(d20) 4.03(d11) (DPPC)	
(Guler et al., 2009)	48 (DPPC)		64 (DPPC)	1229 (DPPC)	38.4 (DPPC)				
(Bunge et al., 2008)	40					16.2*			0.221
(Bartels et al., 2008)	20		43.8+			19.8			
	30					19.1			
	45					16.2			~0.25
	60					14.9			~0.22
(ThisWork, 2018)	3	---	44.5	1099*	49.4	---	30.4	3.95(d20) 4.14(d11)	
(ThisWork, 2018)	45	37.6	64	1172*	36.6	13.3			

*Some assumptions, or calculated from other quantities, +Assumed tilt = 0 degrees.

Table S3. Summary of structural parameters from ESM experiments

	T (°C)	D _{PP} (Å)	A _L (Å ²)	Volume (Å ³)	D _B (Å)	D _C (Å)	Tilt (°)	d-space (Å)	<S _{CH} >
(Chachatry et al., 2005)	20							4.2	
	50							4.6	
(Chemin et al., 2008)	20		40.2+					4.17	
	55				~48				
(Quinn and Wolf, 2009)	20	42.1(ave)					0	4.21	
	50	39.6(ave)				17.3			
(Leftin et al., 2014)	48		53.2 (ave)		49.9(D _B) (ave)	17.0 (ave)			~0.32
(ThisWork, 2018)	45	38.6	64	1187	37.1	13.6			

+Assumed tilt = 0 degrees.

References for Supplementary Material

- Ahmad, T.Y., Sparrow, J.T., Morrisett, J.D., 1985. Fluorine-labeled, pyrene-labeled, and nitroxide-labeled sphingomyelin - Semi-synthesis and thermotropic properties. *J Lipid Res* 26, 1160-1165.
- Bar, L.K., Barenholz, Y., Thompson, T.E., 1997. Effect of sphingomyelin composition on the phase structure of phosphatidylcholine-sphingomyelin bilayers. *Biochemistry-U.S.* 36, 2507-2516.
- Barenholz, Y., Shinitzky, M., 1976. Effect of Sphingomyelin Level on Membrane Dynamics. *Israel J Med Sci* 12, 1362-1363.
- Barenholz, Y., Suurkuusk, J., Mountcastle, D., Thompson, T.E., Biltonen, R.L., 1976. A calorimetric study of thermotropic behavior of aqueous dispersions of natural and synthetic sphingomyelins. *Biochemistry-U.S.* 15, 2441-2447.
- Bartels, T., Lankalapalli, R.S., Bittman, R., Beyer, K., Brown, M.F., 2008. Raftlike mixtures of sphingomyelin and cholesterol investigated by solid-state H-2 NMR spectroscopy. *J Am Chem Soc* 130, 14521-14532.
- Bunge, A., Muller, P., Stockl, M., Herrmann, A., Huster, D., 2008. Characterization of the ternary mixture of sphingomyelin, POPC, and cholesterol: Support for an inhomogeneous lipid distribution at high temperatures. *Biophys J* 94, 2680-2690.
- Calhoun, W.I., Shipley, G.G., 1979a. Fatty-acid composition and thermal-behavior of natural sphingomyelins. *Biochimica et biophysica acta* 555, 436-441.
- Calhoun, W.I., Shipley, G.G., 1979b. Sphingomyelin-lecithin bilayers and their interaction with cholesterol. *Biochemistry-U.S.* 18, 1717-1722.
- Chachaty, C., Rainteau, D., Tessier, C., Quinn, P.J., Wolf, C., 2005. Building up of the liquid-ordered phase formed by sphingomyelin and cholesterol. *Biophys J* 88, 4032-4044.
- Chemin, C., Bourgaux, C., Pean, J.M., Pabst, G., Wuthrich, P., Couvreur, P., Ollivon, M., 2008. Consequences of ions and pH on the supramolecular organization of sphingomyelin and sphingomyelin/cholesterol bilayers. *Chem Phys Lipids* 153, 119-129.
- Chien, K.Y., Huang, W.N., Jean, J.H., Wu, W.G., 1991. Fusion of sphingomyelin vesicles induced by proteins from Taiwan cobra (*Naja-Naja Atra*) venom - Interactions of zwitterionic phospholipids with cardiotoxin analogs. *J Biol Chem* 266, 3252-3259.
- Estep, T.N., Mountcastle, D.B., Barenholz, Y., Biltonen, R.L., Thompson, T.E., 1979. Thermal-behavior of synthetic sphingomyelin-cholesterol dispersions. *Biochemistry-U.S.* 18, 2112-2117.
- Filippov, A., Oradd, G., Lindblom, G., 2006. Sphingomyelin structure influences the lateral diffusion and raft formation in lipid bilayers. *Biophys J* 90, 2086-2092.
- Garcia-Arribas, A.B., Axpe, E., Mujika, J.I., Merida, D., Busto, J.V., Sot, J., Alonso, A., Lopez, X., Garcia, J.A., Ugalde, J.M., Plazaola, F., Goni, F.M., 2016. Cholesterol-ceramide interactions in phospholipid and sphingolipid bilayers as observed by positron annihilation lifetime spectroscopy and molecular dynamics simulations. *Langmuir : the ACS journal of surfaces and colloids* 32, 5434-5444.
- Guler, S.D., Ghosh, D.D., Pan, J., Mathai, J.C., Zeidel, M.L., Nagle, J.F., Tristram-Nagle, S., 2009. Effects of ether vs. ester linkage on lipid bilayer structure and water permeability. *Chem Phys Lipids* 160, 33-44.
- Jimenez-Rojo, N., Garcia-Arribas, A.B., Sot, J., Alonso, A., Goni, F.M., 2014. Lipid bilayers containing sphingomyelins and ceramides of varying N-acyl lengths: a glimpse into sphingolipid complexity. *Biochimica et biophysica acta* 1838, 456-464.
- Kodama, M., Kawasaki, Y., Ohtaka, H., 2012. The main transition enthalpy of the gel-to-liquid crystal phases for a series of asymmetric chain length D-erythro (2S, 3R) sphingomyelins. *Thermochim Acta* 532, 22-27.
- Leftin, A., Molugu, T.R., Job, C., Beyer, K., Brown, M.F., 2014. Area per lipid and cholesterol interactions in membranes from separated local-field C-13 NMR spectroscopy. *Biophys J* 107, 2274-2286.

Li, X.M., Smaby, J.M., Momsen, M.M., Brockman, H.L., Brown, R.E., 2000. Sphingomyelin interfacial behavior: The impact of changing acyl chain composition. *Biophys J* 78, 1921-1931.

Mannock, D.A., McIntosh, T.J., Jiang, X., Covey, D.F., McElhaney, R.N., 2003. Effects of natural and enantiomeric cholesterol on the thermotropic phase behavior and structure of egg sphingomyelin bilayer membranes. *Biophys J* 84, 1038-1046.

Maulik, P.R., Atkinson, D., Shipley, G.G., 1986. X-ray-scattering of vesicles of N-acyl sphingomyelins - Determination of bilayer thickness. *Biophys J* 50, 1071-1077.

Maulik, P.R., Shipley, G.G., 1996. N-palmitoyl sphingomyelin bilayers: Structure and interactions with cholesterol and dipalmitoylphosphatidylcholine. *Biochemistry-Us* 35, 8025-8034.

Mckeone, B.J., Pownall, H.J., Massey, J.B., 1986. Ether phosphatidylcholines - Comparison of miscibility with ester phosphatidylcholines and sphingomyelin, vesicle fusion, and association with apolipoprotein-a-I. *Biochemistry-Us* 25, 7711-7716.

Mehnert, T., Jacob, K., Bittman, R., Beyer, K., 2006. Structure and lipid interaction of N-palmitoylsphingomyelin in bilayer membranes as revealed by H-2-NMR spectroscopy. *Biophys J* 90, 939-946.

Nyholm, T.K.M., Nylund, M., Slotte, J.P., 2003. A calorimetric study of binary mixtures of dihydrosphingomyelin and sterols, sphingomyelin, or phosphatidylcholine. *Biophys J* 84, 3138-3146.

Quinn, P.J., Wolf, C., 2009. Thermotropic and structural evaluation of the interaction of natural sphingomyelins with cholesterol. *Biochimica et biophysica acta* 1788, 1877-1889.

Ramstedt, B., Slotte, J.P., 1999. Comparison of the biophysical properties of racemic and d-erythro-N-acyl sphingomyelins. *Biophys J* 77, 1498-1506.

Shaw, K.P., Brooks, N.J., Clarke, J.A., Ces, O., Seddon, J.M., Law, R.V., 2012. Pressure-temperature phase behaviour of natural sphingomyelin extracts. *Soft matter* 8, 1070-1078.

Sripada, P.K., Maulik, P.R., Hamilton, J.A., Shipley, G.G., 1987. Partial synthesis and properties of a series of N-acyl sphingomyelins. *J Lipid Res* 28, 710-718.

ThisWork, 2018.